THE JOURNAL OF BIOLOGICAL CHEMISTRY VOL. 287, NO. 26, pp. 22328–22340, June 22, 2012

Sperm Epidermal Growth Factor Receptor (EGFR) Mediates α7 Acetylcholine Receptor (AChR) Activation to Promote Fertilization

Received for publication, August 10, 2011, and in revised form, May 9, 2012 Published, JBC Papers in Press, May 10, 2012, DOI 10.1074/jbc.M111.292292

Yael Jaldety[‡], Yair Glick[‡], Avi Orr-Urtreger[§¶], Debby Ickowicz[‡], Doron Gerber[‡], and Haim Breitbart[‡1]

From [‡]The Mina and Everard Goodman Faculty of Life Sciences, Bar-Ilan University, Ramat-Gan 52900, Israel, the [§]Genetics Institute, Tel Aviv Sourasky Medical Center, Tel Aviv, Israel, and the [¶]Sackler Faculty of Medicine, Tel Aviv University, Tel Aviv 69978, Israel

Background: The acrosome reaction is a process that allows sperm penetration into the egg and fertilization.
Results: α7nAChR and EGFR interact with the egg zona pellucida leading to the acrosome reaction.
Conclusion: The EGFR mediates the acrosome reaction induced by α7nAChR activation.
Significance: This finding leads to a better understanding of the signaling that mediates fertilization.

To attain fertilization the spermatozoon binds to the egg zona pellucida (ZP) via sperm receptor(s) and undergoes an acrosome reaction (AR). Several sperm receptors have been described in the literature; however, the identity of this receptor is not yet certain. In this study, we suggest that the α7 nicotinic acetylcholine receptor (α7nAChR) might be a sperm receptor activated by ZP to induce epidermal growth factor receptor (EGFR)-mediated AR. We found that isolated ZP or α7 agonists induced the AR in sperm from WT but not α7-null spermatozoa, and the induced AR was inhibited by α7 or EGFR antagonists. Moreover, α7-null sperm showed very little binding to the egg, and microfluidic affinity *in vitro* assay clearly showed that α7nAChR, as well as EGFR, interacted with ZP3. Induction of EGFR activation and the AR by an α7 agonist was inhibited by a Src family kinase (SFK) inhibitor. In conclusion we suggest that activation of α7 by ZP leads to SFK-dependent EGFR activation, Ca^{2+} influx, and the acrosome reaction.

Ejaculated mammalian spermatozoa must reside in the female genital tract for several hours before gaining the ability to fertilize the egg. Apparently, sperm cells undergo some physiological and biochemical changes, collectively called capacitation, that render the spermatozoa capable of fertilization. During mammalian fertilization, the capacitated spermatozoon penetrates the cumulus oophorous of the ovum and then binds to the zonae pellucidae (ZP)[2] with its plasma membrane intact. Zona binding induces the sperm cell to undergo the acrosomal reaction, which involves multiple fusions between the outer acrosomal membrane and the overlying plasma membrane. However, a recent publication argues against this paradigm, suggesting that sperm that undergo acrosome reaction before reaching the egg can penetrate and fertilize the egg (1). It has been shown that ZP3 or crude extract of ZP can cause sustained elevation in $[Ca^{2+}]_i$ in bovine, mouse, or hamster sperm (2–5). ZP3 triggers the elevation of $[Ca^{2+}]_i$ by activating voltage-gated Ca^{2+} channel, possibly a member of the Cav3 family (6). Two members of this family, Cav3.1 and 3.2, are present in the sperm head and may mediate the acrosome reaction (7–11). However, disruption of the genes that encode for these channels does not affect fertility (11, 12), suggesting that neither of these channels alone is essential for sperm function. It also has been suggested that ZP3 activates TRPC2 (canonical transient receptor potential) via a store-operated mechanism (13, 14), although Ca^{2+} entry is not inhibited by blocking TRPC2 (13) suggesting that other channels may contribute to Ca^{2+} influx. Moreover, disrupting the *trpc2* gene in mice does not affect fertility (15). These data suggest that other calcium channels besides Cav3 and TRPC2 account for Ca^{2+} entry.

The nicotinic acetylcholine receptors are ligand-gated cation channels found mainly in neurons and in skeletal muscle. Most nAChRs are heteropentamers with various combinations of α- and β-subunits, except for the α-bungarotoxin-sensitive α7, α8, and α9, which form homomeric channels (16, 17). Several proteins are associated with nAChR, including rapsyn, which mediates the association of the receptor to the cytoskeleton (18–20). Protein tyrosine phosphorylation mediates the cytoskeletal anchoring of the receptor (21, 22), and SFK are involved in this phosphorylation (23). Inhibition of Src increases the response of the receptor, and vice versa, when Src is highly activated the receptor activity is inhibited (24). α7nAChR is known to be active in Ca^{2+} transport (25), and it can also elevate intracellular calcium levels through the phospholipase C and inositol 1,4,5-trisphosphate pathways and not through channel activity (26).

Several reports suggest that nAChRs are present in mammalian sperm (27–29). Acetylcholine esterase and acetylcholine transferase are found in ram, rat, and human sperm (30, 31). Moreover, a cholinergic receptor has been identified in ram sperm (32). It has been shown that α7nAChR is involved in the zona pellucida-induced acrosome reaction (33, 34) and that α7-null sperm have impaired motility (35). It also has been found that acetylcholine (ACh) increases intracellular calcium levels (36). Moreover, the α7 subunit is associated with SFK in

[1] To whom correspondence should be addressed. Tel.: 972-3-5318201; Fax: 972-3-6356041; E-mail: haim.breitbart@biu.ac.il.

[2] The abbreviations used are: ZP, zona pellucida; ACh, acetylcholine receptor; α7nAChR, α7 nicotinic acetylcholine receptor; SFK, Src family kinase; EGFR, epidermal growth factor receptor; AR, acrosome reaction; IVF, *in vitro* fertilization; α-BgT, α-bungarotoxin; MLA, methyllycaconitine; PNU, PNU282987; 8-Br-cAMP, 8-bromo-cyclic AMP.

human sperm and inhibitors of tyrosine phosphatases inhibit the ACh-induced acrosome reaction (37). In neurons α7 is associated with actin (38), suggesting a role for this subunit in actin remodeling. We have shown that F-actin is formed in sperm capacitation; this F-actin network must be depolymerized in order to achieve the acrosome reaction (39, 40). Thus, α7 also may be an important signaling molecule in sperm capacitation.

Epidermal growth factor receptors (EGFRs) are receptor tyrosine kinases and are activated by a large family of peptidic ligands that induce the formation of active auto (trans)-phosphorylated receptor homo-/heterodimers. The active dimers, upon recruitment of adaptor and signaling proteins, initiate multiple signaling events (41–45). G protein-coupled receptor signaling is mediated by receptor tyrosine kinases such as EGFR in a process called transactivation (46–49), a mechanism that exists in sperm as well (50). The activation of the EGFR generates a Ca^{2+} signal, broadly defined as the transient rise of the intracellular concentration of Ca^{2+} (51). We showed previously that bovine sperm contains EGFR localized to the sperm head and the mid-piece (50, 52). It also has been shown that EGFR is involved in the AR and in actin polymerization during sperm capacitation (39, 50, 52). Moreover, EGFR phosphorylation/activation is increased during capacitation. Further stimulation of the EGFR in capacitated sperm reveals increased intracellular calcium levels leading to AR (50).

It is well established that Src kinase is a known activator of the EGFR (53). The fact that Src kinase co-localizes with α7 in human sperm and antagonists of tyrosine phosphorylation inhibit the acetylcholine-initiated acrosome reaction (37) supports the notion of a possible cross-talk between α7 and the EGFR.

The aim of the present study was to investigate the role and mechanism of sperm α7nAChR in the acrosome reaction and fertilization processes. We show that α7 mediates calcium influx, acrosome reaction, and sperm-egg binding. Moreover, our data reveal for the first time that these processes are mediated by the Src/EGFR system.

EXPERIMENTAL PROCEDURES

Materials

Calcium Ionophore A23187 and protease inhibitor mixture were obtained from Calbiochem. Fluo-4/AM was obtained from Fluka. Rabbit polyclonal anti- α7 (ab10096), mouse monoclonal anti-EGFR (ab30), rabbit monoclonal anti-EGFR (ab2430-1), and rabbit polyclonal anti-phospho-EGFR Tyr-845 (ab5636) were obtained from Abcam. Mouse anti-tubulin was purchased from Sigma. Goat anti-rabbit IgG (H+L)-HRP conjugate and goat anti-mouse IgG (H+L)-HRP conjugate were obtained from Bio-Rad. Goat anti-rabbit IgG (H+L)-Alexa Fluor 568 was purchased from Molecular Probes (Leiden, The Netherlands). All other chemicals were purchased from Sigma unless otherwise stated.

Mouse Sperm Preparation and Capacitation

Sexually mature male mice (C57) were sacrificed by CO_2 asphyxiation. The pair of cauda epididymides and part of the vas deferens were rapidly removed and minced in 0.5 ml of HM medium (modified Krebs-Ringer bicarbonate medium (54)). The sperm were released from the epididymal lumen for 5 min at 37 °C. The medium was carefully collected, and the cells were washed by centrifugation (780 × *g*, 5 min) in the same medium and then left for swim-up for 5 min at 37 °C. The motile fraction was carefully collected, and the washed cells were counted and maintained at 37 °C until use.

Capacitation of mouse epididymal sperm (1×10^7 cells/ml) was induced as described previously (54). Briefly, sperm pellets were resuspended to a final concentration of 10^7 cells/ml in HMB medium (containing 119.4 mM NaCl, 4.8 mM KCl, 1.7 mM $CaCl_2$, 1.2 mM $MgSO_4$, 10 mM $NaHCO_3$, 25 mM Hepes, pH 7.4, 25 mM sodium lactate, 5.56 mM glucose, 0.001% phenol red, 10 IU/ml penicillin, and 3 mg/ml BSA). The cells were incubated in this capacitation medium for 1.5 h at 37 °C with 5% CO_2.

Assessment of Mouse Sperm Acrosome Reaction

An aliquot of spermatozoa (10^5 cells) was smeared on a glass slide and allowed to air-dry. Spermatozoa were then permeabilized by methanol for 15 min at room temperature, washed three times at 5-min intervals with 25 mM Tris-buffered saline, pH 7.6 (TBS), and air-dried. FITC-conjugated peanut lectin agglutinin was put on air-dried spermatozoa smears to trace microscopically acrosome-reacted spermatozoa. Cells were incubated with FITC-conjugated peanut lectin agglutinin (12.5 μg/ml in TBS) for 0.5 h, washed with H_2O, and mounted with FluoroGuard Antifade (Bio-Rad). For each experiment, at least 200 cells/slide on duplicate slides were evaluated (total of 400 cells for one experiment). Cells with green staining over the acrosomal cap were considered acrosome intact; those with equatorial green staining or no staining were considered acrosome reacted.

Isolation of Zonae Pellucidae

Zonae pellucidae were ovarian homogenates as described earlier by Bleil and Wassarman (56). Briefly, large numbers of zonae pellucidae ($5–20 \times 10^3$) were isolated by Percoll gradient centrifugation of ovarian homogenates. Ovaries dissected from 20–30 mice (21 days old) were homogenized on ice in 4 ml of a buffer containing 25 mM triethanolamine, pH 8.5, 150 mM NaC1, 1 mM $MgC1_2$, and 1 mM $CaCl_2$ to which 1 mg of DNase and 1 mg of hyaluronidase were added. The homogenate was brought to 1% Nonidet P-40 and 0.1 mM phenylmethylsulfonyl fluoride and subjected to about 10 more strokes of the pestle. The homogenate was then brought to 1% deoxycholate, mixed with 9 ml of homogenization buffer containing Percoll (72%) in a seal-cap tube, and centrifuged at 25,000 rpm for 45 min at 4 °C in a rotor. Under these conditions, zona pellucida appeared as a narrow, opaque band at a density of 1.02 g/ml.

In Vitro Fertilization (IVF) and Detection of Sperm-Egg Binding

Female (C57BI×A.G) mice, 6–8 weeks old, were superovulated with 5 IU of pregnant mare's serum gonadotropin followed at a 48-h interval by 5 IU of human chorionic gonadotropin and killed between 12 and 17 h after the human chorionic gonadotropin injection. Oocytes were liberated from the ampullae into M16 medium (Sigma Cat. No. M7292). Mouse epididymal sperm (1×10^7 cells/ml) were prepared and capac-

itated as described. A sample of 10^5 sperm cells was added and incubated in a 100-μl droplet (on average 15–25 eggs were present in each droplet for each experiment) at 37 °C in 5% CO_2 for 24 h. Then the eggs were examined under ×50 magnification of a dissecting microscope to determine the number of 1-cell and 2-cell eggs present. The whole experiment was repeated three times. For the sperm-egg binding assay, oocytes were transferred to a glass slide after 4–5 h of incubation to estimate bound sperm under the microscope.

Immunoblot Analysis

Sperm lysates were prepared by the addition of lysis buffer (containing 6% SDS, 1 M Tris-HCl, pH 7.5, 1 mM sodium orthovanadate, 1 mM benzamidine, 50 mM sodium fluoride, 0.1 M sodium pyrophosphate, 1:100 protease inhibitor mixture, and 1 mM PMSF) for 15 min and then centrifuged at 10,000 × *g* at 4 °C. 5× sample buffer was added to the supernatant and boiled for 5 min. The extracts were separated on 10% SDS-polyacrylamide gels and then transferred electrophoretically to nitrocellulose membranes (200 mA, 2 h) using a buffer composed of 25 mM Tris, pH 8.2, 192 mM glycine, and 20% methanol. For Western blotting, nitrocellulose membranes were blocked with 5% BSA in Tris-buffered saline, pH 7.6, containing 0.1% Tween 20 (TBS-T) for 30 min at room temperature. The membranes were incubated overnight at 4 °C with the primary antibodies. Next, the membranes were washed three times with TBS-T and incubated for 1 h at room temperature with specific HRP-linked secondary anti-rabbit or anti-mouse antibody (Bio-Rad) diluted 1:5000 in TBS-T. The membranes were washed three times with TBS-T and visualized by enhanced chemiluminescence (Amersham Biosciences).

Determination of Mouse Intracellular Calcium

The intracellular concentration of free Ca^{2+} was assessed using the fluorescent calcium indicator Fluo-4/AM. Washed cells (1×10^7/ml) were incubated in HMB for 30 min, and then 1 μM Fluo-4/AM was added for a further 1 h. The loaded cells were then washed three times to remove extracellular Fluo-4/AM. The cells were used immediately for fluorescence measurements using a plate reader with an excitation wavelength of 485 nm and emission of 535 nm. During fluorescence measurements, sperm suspensions were maintained at 37 °C.

Immunocytochemistry

Anti-EGFR and anti-α7nAChR antibodies were used at a 1:50 dilution on permeabilized sperm smears to determine intracellular localization of proteins as described previously (57). Nonspecific staining was determined by incubating the sperm in the presence of goat anti-rabbit IgG (H+L)-Alexa Fluor 568 alone diluted at 1:200, and no staining was detected.

Microscopy

All images were captured on an Olympus AX70 microscope at a magnification of ×400. This microscope was equipped with an Olympus DP50 digital camera and with Viewfinder Lite software (version 1 from Pixera Corp., Los Gatos, CA). All fluorescence determinations were done under nonsaturated conditions. Each experiment and staining were performed on the same day, and sperm were photographed within 24 h to reduce fading. All cell preparations from a single experiment were photographed during the same session and at the same exposure time.

Immunoprecipitation

Proteins extracted from spermatozoa (5×10^7) using triple detergent homogenization buffer consisting of 0.5% deoxycholate, 2% Triton X-100, 0.2% SDS, 50 mM NaCl, 5 mM Tris-HCl, pH 7.5, 1 mM Na_3VO_4, 1 mM benzamidine, 1:100 protein inhibitor mixture, and 1 mM PMSF were then sonicated at 40 Hz, three times for 10 s each. The tube was then rotated in 4 °C for 30 min, and the cell debris was precipitated by centrifugation at 14,000 rpm for 5 min. The lysate was precleared with protein A/G for 1 h with rotation at 4 °C. The beads were removed after centrifugation. Protein aliquots were incubated with anti-α7nAChR or anti-EGFR (ab30) antibodies overnight at 4 °C. Then 60 μl of protein A/G was added for 5 h with rotation at 4 °C. The immunoprecipitates were collected by centrifugation and washed four times (7500 rpm, 10 min) with TBS containing 0.1% Triton X-100. The final pellet was resuspended in sample buffer and boiled for 5 min before analyzing it on SDS-PAGE and Western blotting as described above.

Microfluidic Affinity Assay

Production of Human Synthetic Genes via Assembly PCR—Synthetic linear human genes were generated by using a two-step assembly PCR. As a template for the first PCR, an *Escherichia coli* clone (in 96-well plates) containing an ORF within the gateway donor plasmids (pENTR223, Invitrogen) was used. A hot start high-fidelity DNA polymerase (Phusion II, Finnzymes) was used for all PCR procedures. In the first PCR step, epitope tags (c-Myc in the N terminus and His tag in the C terminus) were added to α7, AZGP1, and SERPINA1 proteins, and T7 tags were added to ZP3 protein. No tags were added to EGFR-eGFP. The tags were added by using the primers 5′-GW223-cMyc and 3′-GW223-His, 5′GW223, and 3′-GW223-T7 or 5′-GW223 and 3′-GW223. A reaction mix with a total volume of 20 μl was prepared using 0.8 unit of DNA polymerase for each reaction. The PCR assay was performed in 25 cycles with annealing temperature of 64 °C. The extension time ranged between 45 and 90 s at 72 °C depending on the ORF length. The first PCR product served as a template for the second PCR. In addition, two different pairs of primers were used for the second PCR step adding the 5′-UTR (T7 promoter) and 3′-UTR (T7 terminator) for each gene. The reaction mixture, with a total volume of 50 μl, was prepared containing 1.5 units of DNA polymerase. The first extension primer pair, containing 85 and 95 bp, was added to the mixture at a low concentration (2.5 nM). After 10 cycles the second primer pair (5′-final and 3′-final) was added to the PCR mixture (0.2 μM) for an additional 25 cycles, completing the PCR process. The PCR products were filtered in multi-well 10K filter plates (AcroPrep™, Pall) and eluted with 40 μl of Double Distilled Water. The gene product yield was verified twice, at the end of the first PCR step and after filtration by 1.5% agarose-gel electrophoresis. In addition, PCR products were transferred to 384 UV-readable plates

and the concentration was measured using a UV plate reader (Synergy™ 4 Hybrid Microplate Reader, BioTek).

Device Fabrication—The microfluidic devices (58) were fabricated on silicone molds casting silicone elastomer polydimethylsiloxane (Sylgard 184, Dow Corning). Each device consists of two aligned polydimethylsiloxane layers, *e.g.* the flow and the control layer. The molds were first exposed to chlorotrimethylsilane (Sigma-Aldrich) vapor for 10 min to promote elastomer release after the baking steps. A mixture of a silicone-based elastomer and curing agent was prepared in two different ratios, 5:1 and 20:1, for the control and flow molds, respectively. The control layer was degassed and baked for 30 min at 80 °C. The flow layer was initially spin-coated (Laurell Technologies Corp.) at 2500 rpm for 60 s and baked at 80 °C for 30 min. The control layer was separated from its mold, and control channel access holes were punched. Next, the flow and control layers were aligned manually under a stereoscope and baked for 2 h at 80 °C. The two-layer device was peeled from the flow mold, and flow channel access holes were punched. Finally, the microfluidic devices were aligned to epoxy-coated glass substrates (CEL Associates) and bonded overnight on a heated plate at 80 °C.

Surface Chemistry—To prevent nonspecific adsorption and achieve a suitable binding orientation of expressed proteins, all accessible surface area within the microfluidic device was chemically modified. This surface chemical modification also facilitated the self-assembly of a protein array on the surface. Biotinylated BSA (1 μg/μl) was flowed for 20 min through the device, binding the BSA to the epoxy surface. On top of the biotinylated BSA, 0.5 μg/μl streptavidin (Neutravidin, Pierce) was added for 20 min. The "button" valve was then closed and biotinylated BSA was flowed over again (as described above), passivating the rest of the device. Following passivation, the button valve was released, and a flow of 0.2 μg/μl penta-His-biotin (Qiagen) or α-GFP-biotin (Abcam) was applied. The antibody bound to the exposed streptavidin specifically at the area under the button, creating an anti-His tag or anti-GFP array. Hepes (50 mM) was used for washing the unreacted substrate between each of the different surface chemistry steps.

Protein Expression—Proteins were expressed in a test tube using a rabbit reticulocyte quick-coupled transcription and translation reaction (Promega). The expression of the protein in a test tube was performed in a final volume of 25 μl including 1 μg of DNA. Microsomal membranes (Promega) were added for the expression of membrane-bound proteins (59). The tube was incubated at 30 °C for 2.5 h with agitation (600 rpm).

Protein Pulldown—Expressed proteins were then diffused through to the reaction chamber binding their His tag/GFP to the anti-His/GFP antibody under the button valve, thus immobilizing the protein. Proteins were labeled with an anti-C-Myc Cy3 antibody, which bound to its corresponding epitope located at the protein N terminus and labeled it. Protein expression levels were determined with a microarray scanner (LS Reloaded, Tecan) using a 532-nm laser and 575-nm filter (Cy3) or a 488-nm laser and 535-nm filter (GFP).

Protein Network Interaction Generator (PING) (60)—ZP3 were expressed in a tube, as described above, and flowed over the device. By closing the "sandwich" valves, each unit cell separated from its environment. Next the button valves opened, exposing the pulled down proteins on the device. The device was incubated for 30 min at room temperature. Proteins were labeled with α-T7 Cy5 antibody (Abcam), which bound to its corresponding epitope located at the ZP3 N terminus and labeled it. Protein interactions were determined with a microarray scanner (LS Reloaded, Tecan) using a 633-nm laser and 695-nm filter for Cy5.

Statistical Analysis

Data are expressed as mean ± S.D. of at least three experiments. Statistical significance was assessed between groups using Student's *t* test, and differences of $p > 0.05$ were considered significant.

RESULTS

Involvement of α7nAChR in ZP-induced Acrosome Reaction—ACh has a role in follicle maturation in the female reproductive system (61–63). It is also known that AChRs exist in sperm and that its ligand, ACh, increases sperm motility and intracellular calcium levels (31, 32, 34, 36). Moreover, it has been shown that α7nAChR participates in the acrosome reaction (33, 34, 64). In the present study, we examined the mechanism by which α7nAChR activates the AR and its importance in initiating the process. To establish the involvement of α7nAChR in the AR process, we examined the effect of PNU282987 (*N*-[(3*R*)-1-azabicyclo[2.2.2]oct-3-yl]-4-chlorobenzamide hydrochloride), a specific agonist of α7nAChR (65), on the AR rate. In Fig. 1*A* shows that PNU282987 can indeed elevate the AR rate; the specific inhibitors α-bungarotoxin (α-BgT) and methyllycaconitine (MLA) diminish this effect in a concentration-dependent manner. Interestingly, acrosome reaction induced by isolated ZP was also inhibited by BgT and MLA (Fig. 1, *A* and *B*), indicating a role for α7nAChR in the physiological AR. Acrosome reaction is significantly enhanced by ACh, the ligand of nAChR, and this effect was highly inhibited by the specific inhibitors α-BgT and MLA (Fig. 1*B*). Interestingly, a synergistic effect was seen when ZP and PNU were added together at relatively low concentrations (1.5 egg ZP/μl and 1 μM PNU, respectively) (Fig. 1*C*). Furthermore, ACh, PNU, ZP, phorbol 12-myristate 13-acetate (protein kinase C activator), 8-Br-cAMP (protein kinase A and Epac activator), and the Ca^{2+}-ionophore A23187 each managed to induce the AR at a significant rate in the WT but not in α7nAChR-null mice, except for the Ca^{2+}-ionophore (Fig. 1*D*). These data suggest a crucial role for α7nAChR in the AR process. Moreover, the ability of the Ca^{2+}-ionophore to induce the AR in α7-null sperm suggests that α7nAChR mediates Ca^{2+} transport into the cells. To test whether α7nAChR is involved in sperm capacitation, the cells were incubated under capacitation conditions in the presence of α-BgT or MLA, and their effect on the Ca^{2+}-ionophore-induced AR was determined. No effect of these inhibitors on the AR rate was observed (Fig. 2*A*). In addition, the pattern of protein tyrosine phosphorylation as a known marker for capacitation was examined in α7-null sperm. Fig. 2*B* shows that there are no significant differences between the control and the null sperm phosphorylation pattern, indicating that the α7 receptor is not involved in the capacitation process. To show the importance of α7nAChR in the fertilization process, we evaluated the rate

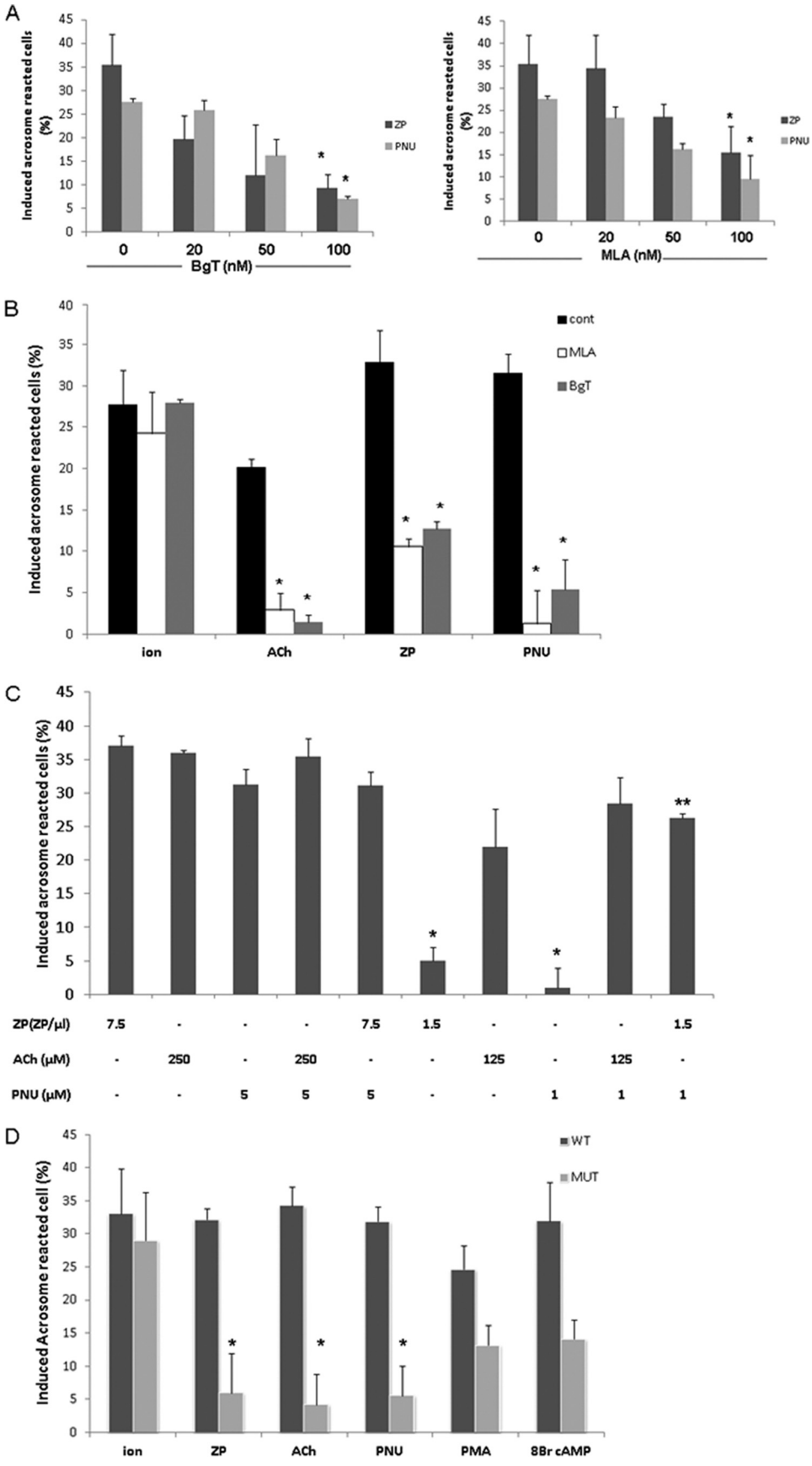
A
Induced acrosome reacted cells (%)
ZP
PNU
BgT (nM)
MLA (nM)
B
Induced acrosome reacted cells (%)
cont
MLA
BgT
ion
ACh
ZP
PNU
C
Induced acrosome reacted cells (%)
ZP(ZP/μl)
ACh (μM)
PNU (μM)
D
Induced Acrosome reacted cell (%)
WT
MUT
ion
ZP
ACh
PNU
PMA
8Br cAMP

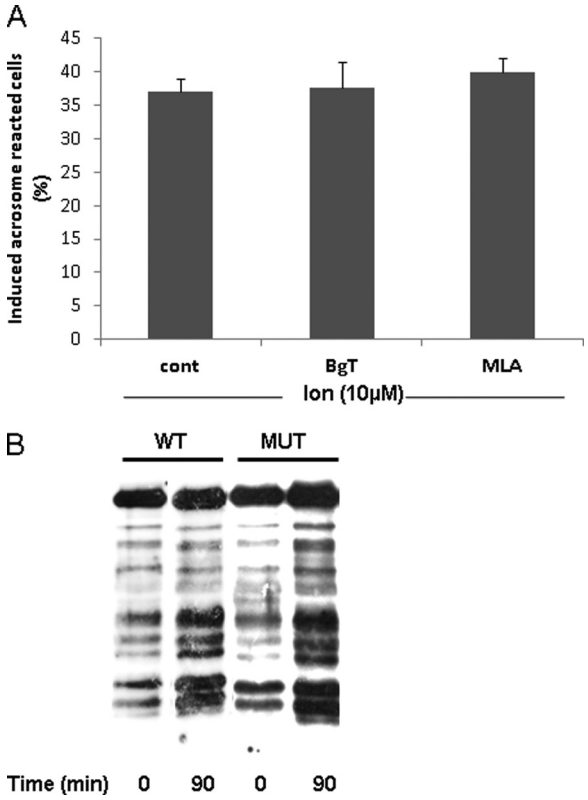

FIGURE 2. **Involvement of α7nAChR in capacitation.** Sperm from WT or α7-null mice (*MUT*) (*B*) were incubated in capacitation medium for 1.5 h in the presence or absence of α-BgT (100 nM) or MLA (100 nM) (*A*). Ca^{2+}-ionophore (*ion*) (A23187, 10 μM) was added for an additional 30 min. At the end of the incubation time, sperm samples were smeared on slides for acrosome reaction determination as described under "Experimental Procedures." The data represent the mean ± S.D. of duplicates from at least three experiments. *B*, sperm proteins were extracted before (0 min) and after (90 min) incubation in capacitation medium with SDS lysis buffer as described under "Experimental Procedures." The extracts were separated on SDS-PAGE and transferred to nitrocellulose membrane that was incubated with anti-phosphotyrosine. The data represent one experiment typical of three repetitions performed. *cont*, control.

TABLE 1

Bound sperm and IVF rate in WT compared with BgT-inhibited cells or α7-null sperm

Sperm from WT or mutant mice (MUT) were incubated in capacitation medium for 1.5 h, and α-BgT (100 nM) was added for the last 30 min. Sperm (10^5) were added to MII oocytes, and the number of sperm bound per egg was counted after 5 h of incubation. The percentage of cleaved oocytes was determined after 24 h of incubation. The data represent the mean ± S.D. from at least three experiments.

Type of sperm	No. of bound sperm	IVF
		%
WT	37.5 ± 10	41.6 ± 8.3
α-BgT	6.6 ± 1.9	29.3 ± 0.7
MUT	2.8 ± 3	22.2 ± 0.5

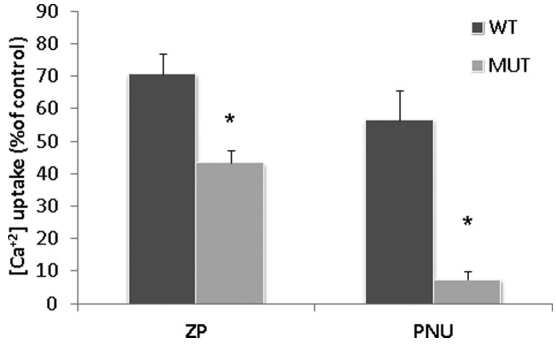

FIGURE 3. **ZP or PNU282987 elevate intracellular calcium levels in WT but not in sperm from a7-null mice.** Sperm from WT or mutant mice (*MUT*) were incubated in capacitation medium for 30 min, then Fluo-4/AM was added for an additional hour. The samples were washed three times in Ca^{2+}-free medium and finally resuspended in a medium containing Ca^{2+}; then they were loaded on 96-wells plate. ZP (~7.5 ZP/μl) or PNU (5 μM) was added, and fluorescence was measured utilizing the TECAN plate reader as described under "Experimental Procedures." Control treatments were also conducted giving the values of 30% of control for ionomycin (10 μM) and 90% for Triton X-100 (0.1% v/v); when EGTA (1 mM) was used there was no effect on intracellular calcium levels. The data represent the mean ± S.D. of duplicates from at least three experiments. *, significant difference from the corresponding control, $p < 0.05$.

of the IVF and sperm binding to the egg in WT and in α-BgT-inhibited and α7-null sperm. Table 1 shows that α7-null sperm and α-BgT-treated sperm had a very low binding ability to the egg. The IVF rate was also reduced in α7-null sperm by 45% compared with the WT sperm (Table 1). These data indicate a role for α7nAChR in sperm-egg binding, indicating that its presence is required for the fertilization process.

It is well accepted that elevation of intracellular Ca^{2+} levels is required to initiate the acrosome reaction (6, 66). Thus, we measured the changes in intracellular Ca^{2+} levels in response to ZP or PNU in WT and α7nAChR-null sperm. Fig. 3 shows that ZP and PNU elevate the intracellular Ca^{2+} levels in WT sperm, whereas in α7nAChR-null sperm there is 40% inhibition in response to ZP and almost complete inhibition in response to PNU (Fig. 3). These data suggest that ZP or PNU activates α7nAChR to induce Ca^{2+} influx. The relatively low inhibition (40%) of the ZP response in α7-null sperm suggests an alternative Ca^{2+} influx pathway, other than α7nAChR, that is activated by ZP. Interestingly, the ZP-induced elevation of intracellular calcium in α7-null sperm is not sufficient to induce the AR (Fig. 1*B*).

EGFR Mediates the Acrosome Reaction Induced by PNU282987 or ZP—We reported previously that EGFR is activated during sperm capacitation, and further activation with EGF at the end of capacitation enhances intracellular calcium levels and the occurrence of AR (50). In two recent publications we further emphasized the role and regulation of EGFR by G protein-coupled receptors and ouabain (50, 68). Hence, we

FIGURE 1. **α7 nicotinic acetylcholine receptor mediates ACh, ZP, or PNU282987 but not calcium Ca^{2+}-ionophore-induced acrosome reaction.** Sperm from WT or α7-null mice (*MUT*) (*D*) were incubated in capacitation medium for 1.5 h. *A*, α-BgT (20–100 nM) or MLA (20–100 nM) was added for the last 30 min of incubation in capacitation medium, and then ZP (~7.5 egg ZP/μl) or PNU (5 μM) was added for an additional 30 min. *B*, α-BgT (100 nM) or MLA (100 nM) was added for the last 30 min of incubation in capacitation medium, and then ACh (250 μM), calcium ionophore (*ion*) (A23187, 10 μM), ZP (~7.5 ZP/μl), or PNU (5 μM) was added for an additional 30 min. *C*, after 1.5 h of incubation in capacitation medium, ZP (~1.5/7.5 ZP/μl), PNU (1/5 μM), or ACh (125/250 μM) was added, as shown on the graph, for an additional 30 min. *D*, after 1.5 h of incubation in capacitation medium, ZP (~1.5 or 7.5 ZP/μl), PNU (1/5 μM), ACh (125/250 μM), phorbol 12-myristate 13-acetate (*PMA*, 100 ng/ml), 8-Br-cAMP (1 mM), or calcium ionophore (A23187, 10 μM) was added for an additional 30 min. Sperm samples were smeared on slides for acrosome reaction determination as described under "Experimental Procedures." The data represent the mean ± S.D. of duplicates from at least three experiments. *, significant difference from the corresponding control (*cont*), $p < 0.05$. **, significant difference from the corresponding inducers (ZP or PNU) $p < 0.05$.

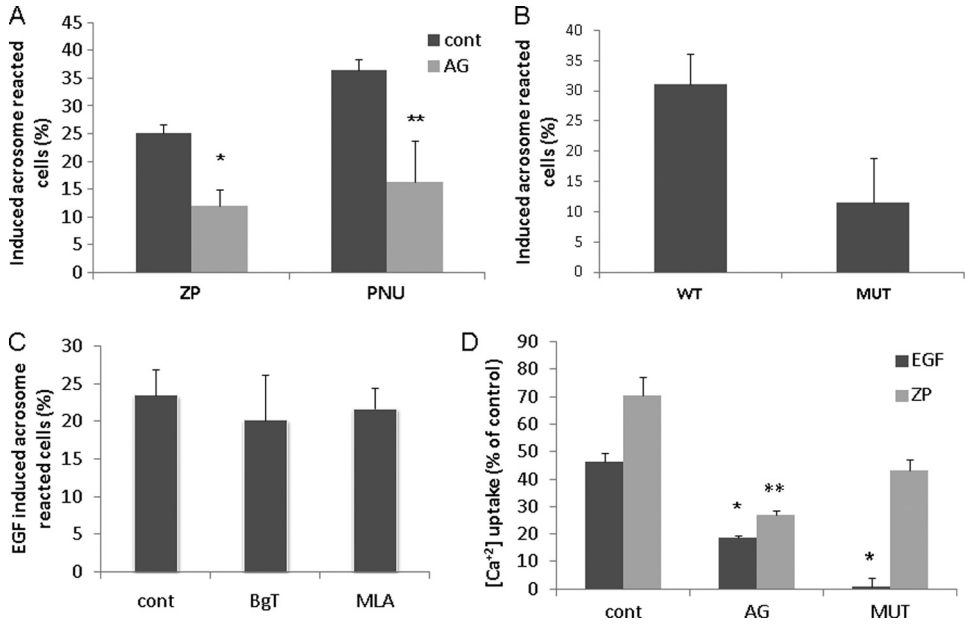

FIGURE 4. **EGFR mediates α7nAChR-activated acrosome reaction.** Sperm from WT or α7-null mice (*B* and *D*, *MUT*) were incubated in capacitation medium for 1.5 h. *A*, AG1478 (*AG*, 10 μM) was added for the last 30 min, and then ZP (~7.5 ZP/μl) or PNU282987 (5 μM) was added for an additional 30 min. *B*, after 1.5 h of incubation in capacitation medium, EGF (1 ng/ml) was added for an additional 30 min. *C*, α-BgT (100 nM) or MLA (100 nM) was added for the last 30 min of incubation in capacitation medium, and then EGF (1 ng/ml) was added for an additional 30 min. Sperm samples were smeared on a slide for acrosome reaction determination. The data represent the mean ± S.D. of duplicates from at least three experiments. *D*, sperm from WT or α7-null mice were incubated in capacitation medium. After 30 min Fluo-4/AM was added for 1 h, and AG1478 (10 μM) was added for the last 30 min. The samples were washed in Ca^{2+}-free medium and finally were resuspended in a medium that contained Ca^{2+}; then they were loaded on 96-wells plate. EGF (1 ng/ml) or ZP (~7.5 ZP/μl) was added, and the fluorescence was measured utilizing the TECAN plate reader as described under "Experimental Procedures." Control treatments (*cont*) were also conducted giving the values of 30% of control for ionomycin (10 μM) and 90% for Triton X-100 (0.1% v/v); when EGTA (1 mM) was used there was no effect on intracellular calcium levels. The data represent the mean ± S.D. of duplicates from at least three experiments. * or **, significant difference from the corresponding control, $p < 0.05$.

hypothesized that the EGFR might mediate the AR induced by ZP. To prove this point, we examined the effect of the specific EGFR inhibitor AG1478 on the ZP-induced AR. The data in Fig. 4*A* show a 50% inhibition in ZP-induced AR in AG1478-treated cells, indicating that EGFR participates in this reaction. Moreover, the data reveal that AR induced by PNU was also 55% inhibited by AG1478 (Fig. 4*A*), suggesting that EGFR mediates AR induced by activation of α7nAChR. When EGF was added to sperm from α7-null mice (Fig. 4*B*), the AR rate of inhibition was 63% compared with WT sperm. Interestingly, EGF-induced AR was not affected by α-BgT or MLA (Fig. 4*C*), suggesting that EGFR is localized downstream to α7nAChR. When Ca^{2+} influx was measured directly in response to EGF, a significant increase in intracellular Ca^{2+} levels was observed in the WT but not in α7nAChR-null sperm (Fig. 4*D*). Moreover, AG1478 inhibited Ca^{2+} influx induced by ZP (Fig. 4*D*). These data suggest that the Ca^{2+} influx induced by ZP is mediated by EGFR and that α7nAChR is required for this process.

To further support the involvement of EGFR in ZP- or PNU-induced AR, the phosphorylation/activation of EGFR was examined in response to ZP or PNU. It is shown (Fig. 5*A*) for the first time that phosphorylation on tyrosine 845 of EGFR was significantly enhanced when ZP or PNU were added to capacitated WT sperm, whereas in α7-null sperm this phosphorylation was not observed. These data further support our notion regarding the involvement of α7nAChR in the mechanism by which ZP and EGF induce the AR. It is known that Src phosphorylates the tyrosine 845 of EGFR, and indeed we found that the SFK inhibitor PP1 inhibits PNU-induced EGFR phosphorylation (Fig. 5*B*). Interestingly, significant inhibition on Tyr-845 phosphorylation was observed by α-BgT, suggesting that α7nAChR is localized upstream to the EGFR (Fig. 5*B*).

SFKs Mediate Activation of EGFR—In a recent study we showed in bovine sperm that the non-receptor tyrosine kinase, Src, mediates the activation of EGFR (50). Moreover, SFK was found in complex with α7nAChR in neurons and in human sperm (24, 37). Also, we found (Fig. 5) that EGFR was phosphorylated on tyrosine 845, a residue that is phosphorylated by Src, and that PP1 blocked this phosphorylation (Fig. 5*B*). Under these circumstances, we assumed that Src might be involved in the mechanism of α7nAChR/EGFR activation. To test this possibility, we used PP1, a specific inhibitor of SFK, and induced AR with ZP, EGF, or PNU282987. Fig. 6*A* shows that PP1 significantly inhibits the AR induced by ZP or PNU282987 and partially inhibits the AR induced by EGF.

We also determined the activation of Src by following its phosphorylation on tyrosine 416 (69). Phosphorylation/activation of Src is increased in response to ZP, EGF, or PNU in the WT but not in α7nAChR-null sperm (Fig. 6*B*). These data support the notion of cross-talk between α7nAChR and EGFR.

Interaction between α7nAChR and EGFR—To strengthen this point, the localization of the α7 and EGF receptors in the sperm was examined. Fig. 7*A* shows that α7nAChR is localized to the acrosome region in sperm from WT mice, and no staining is observed in sperm from α7-null mice. The EGFR is also localized to the acrosome region and to the mid-piece in sperm from WT mice. Surprisingly in sperm from α7-null mice the detection of EGFR revealed very low staining in the acrosome

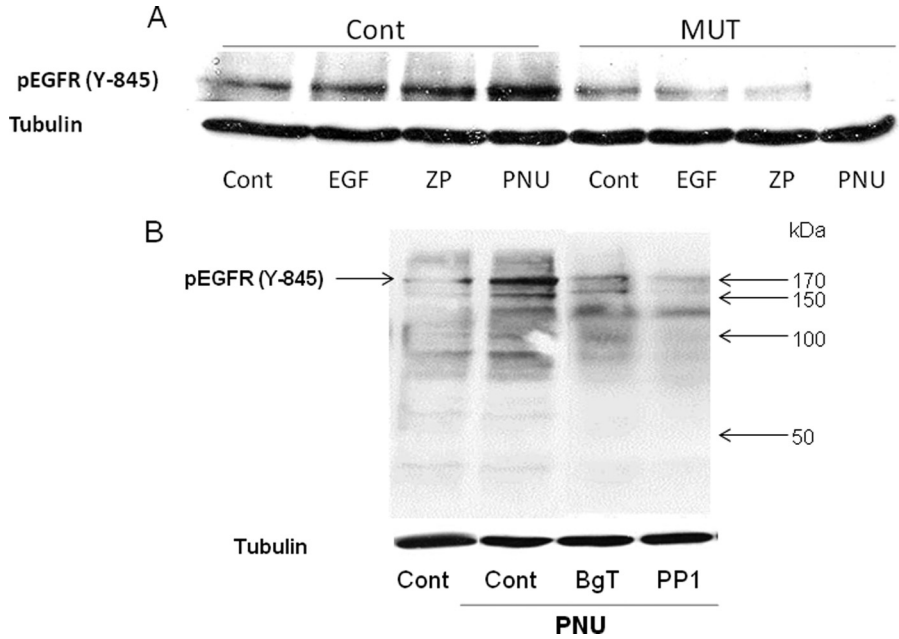

FIGURE 5. **ZP or PNU282987 increase EGFR phosphorylation, which is Src-mediated.** *A*, Sperm from WT (*Cont*) or α7-null mice (*MUT*) were incubated in capacitation medium for 1.5 h. *B*, PP1 (5 μM) or α-BgT (100 nM) was added for the last 30 min of incubation. *A*, EGF (1 ng/ml), ZP (~7.5 ZP/μl), or PNU (in *A* and *B*, 5 μM) was added for an additional 5 min. Sperm proteins were extracted with SDS lysis buffer as described under "Experimental Procedures." The extracts were separated on SDS-PAGE and transferred to nitrocellulose membrane that was incubated with anti-phospho-EGFR (Tyr-845) and with anti-tubulin for protein amount. The data represent one experiment typical of three repetitions performed.

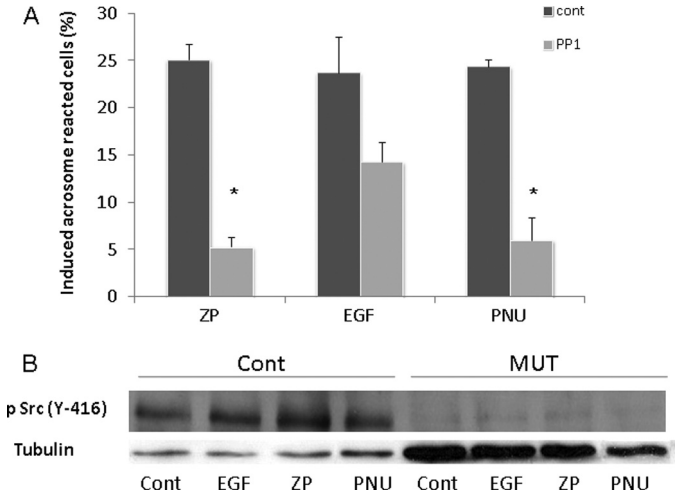

FIGURE 6. **ZP-, EGF-, or PNU282987-induced acrosome reaction is mediated by SFK.** *A*, mouse sperm were incubated in capacitation medium for 1.5 h with PP1 (5 μM) added for the last 30 min; then EGF (1 ng/ml), ZP (~7.5 ZP/μl), or PNU (5 μM) was added for an additional 30 min. Sperm samples were smeared on a slide for acrosome reaction determination as described under "Experimental Procedures." The data represent the mean ± S.D. of duplicates from at least three experiments. *, significant difference from the corresponding control, $p < 0.05$. *B*, mouse sperm from WT (*Cont*) or α7-null mice (*MUT*) were incubated in capacitation medium for 1.5 h, and then PNU (5 μM), EGF (1 ng/ml), or ZP (~7.5 ZP/μl) was added for an additional 5 min. Sperm proteins were extracted with SDS lysis buffer as described under "Experimental Procedures." The proteins were separated on SDS-PAGE and transferred to nitrocellulose membrane, which was incubated with anti-phospho-Src (Tyr-416) and anti-tubulin. The data represent one experiment typical of three repetitions performed.

region, suggesting that the presence of α7nAChR is necessary for the localization of the EGFR to the acrosome. To assess a possible interaction between the two receptors, immunoprecipitation was conducted using anti-EGFR or anti-α7 antibodies. Indeed it is shown that α7nAChR co-immunoprecipitates with the EGFR (Fig. 7*B*). This co-immunoprecipitation was also observed in human neuroblastoma cells (data not shown). When the immunoprecipitation was conducted on α7-null sperm using the anti-α7 antibody, EGFR was not detected by Western blot (Fig. 7*C*). Also, α7 was not detected in a blot performed using α7 mutant sperm (Fig. 7*D*).

To further support the physiological role of α7nAChR and the EGFR in sperm-egg interaction, a microfluidic affinity assay was conducted, confirming the interaction between α7nAChR or EGFR and ZP3. For this matter, α7nAChR, EGFR, or ZP3 was expressed in test tubes; α7nAChR or EGFR-eGFP was then diffused through to the reaction chamber and pulled down to the surface of the device using α-His/α-GFP biotinylated antibodies. The proteins were effectively concentrated under the button valve. Thereafter, ZP3 was flowed through the device and incubated for 30 min. Finally, ZP3 was labeled at the C terminus with α-T7 Cy5 antibody. A scan of the microarray device revealed that ZP3 interacted with EGFR, α7, and the complex of EGFR and α7 co-expressed in the same vesicles. ZP3 did not interact with AZGP1, SERPINA1, or HCV-NS4B, as expected (Fig. 8). The interaction signal is affected by the affinity as well as the amount of protein bound to the surface; therefore, signals were normalized to expression levels and expressed as a ratio normalized to background signals of no protein (Fig. 8, *B* and *D*). The strongest interaction was that of ZP3 with the co-expressed EGFR and α7. This implies a cooperative interaction between ZP3 and an EGFR·α7 complex.

DISCUSSION

The mechanisms regulating sperm acrosome reaction are still not completely understood. Although it was found recently that acrosome-reacted cells can bind to the ZP and fertilize (1), it is accepted that ZP is probably the physiological location at

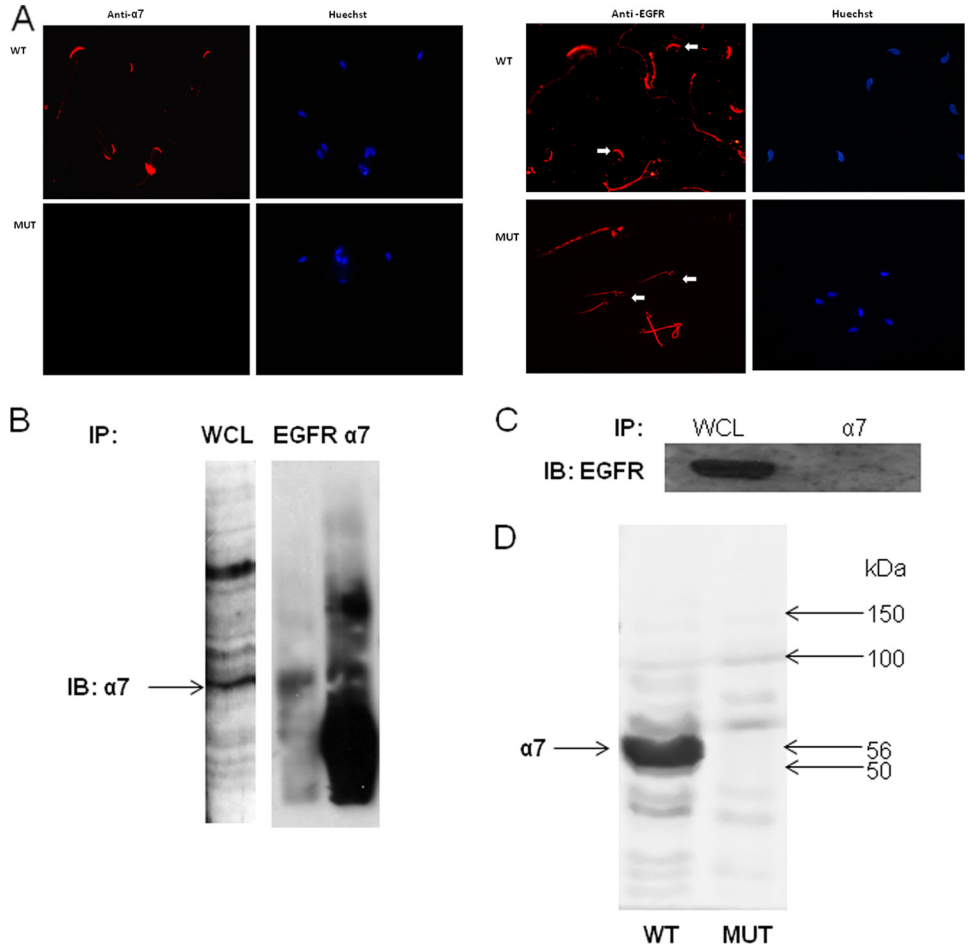

FIGURE 7. **Interaction between α7nAChR and EGFR.** *A*, mouse sperm were smeared on a slide for immunocytochemical staining with anti-α7 or anti-EGFR antibodies as described under "Experimental Procedures." The *arrows* indicate the acrosome. Larger magnification appears in the *upper left corner* of each photograph. Samples of 5×10^7 mouse WT (*B*) or α7-null sperm (*C*) were washed in TBS and resuspended in homogenization buffer. The homogenate was then sonicated at 40 Hz, three times for 10 s each, and rotated at 4 °C for 30 min. The samples were immunoprecipitated (*IP*) and then precleared for 1 h at 4 °C, and antibodies, anti-EGFR (*C*) or anti-α7 (*B* and *D*), were added overnight. The next day, protein A/G was added for 5 h at 4 °C, and the samples were washed four times in TBS containing 0.1% Triton X-100. The washed beads were resuspended in sample buffer, and the sample was boiled for 5 min. The samples were separated in SDS-PAGE as described under "Experimental Procedures," and the membrane was incubated with anti-α7 and goat anti-rabbit secondary antibody or anti-EGFR and goat anti-mouse secondary antibody. The data represent one experiment typical of three repetitions performed. *D*, proteins were extracted from WT or α7-null sperm with SDS lysis buffer as described under "Experimental Procedures." The extracts were separated on SDS-PAGE and were transferred to nitrocellulose membrane that was incubated with anti-α7 as described under "Experimental Procedures." The data represent one experiment typical of three repetitions performed. *IB*, immunoblot; *WCL*, whole cell lysate.

which AR should occur in order to allow sperm penetration into the egg. It is known that binding of the sperm to ZP3 results in fast Ca^{2+} influx into the sperm, a necessary step for the occurrence of the acrosome reaction (70). In the present study we have shown that sperm α7nAChR is crucial for sperm-egg binding and that this receptor has a role in Ca^{2+} influx, which leads to the occurrence of the AR. Moreover, the data indicate that SFK and EGFR mediate these activities. Thus, we describe here for the first time an interesting interaction between α7nAChR and EGFR, which is a necessary step in the mechanism leading to the acrosome reaction.

The first set of experiments was conducted to show that mice sperm contain α7nAChR, which is active in the AR. We showed that activation of α7 by its well known ligand acetylcholine or by the specific α7nAChR agonist PNU282987 caused significant induction of AR, which was inhibited by the specific blockers α-BgT and MLA (Fig. 1, *A* and *B*). Moreover, AR induced by isolated ZP was also inhibited by α-BgT and MLA (Fig. 1, *A* and *B*), indicating that ZP-induced AR is enhanced via activation of α7nAChR. Furthermore, the synergistic effect between ZP and PNU on the AR (Fig. 1*C*) further supports a possible cooperation between α7nAChR and ZP, suggesting that the two pathways are not redundant. The fact that AR induced by the calcium ionophore A23187 is not inhibited by α-BgT or MLA indicates that α7nAChR mediates the AR by activating a pathway leading to Ca^{2+} influx into the sperm. Moreover, we showed that AR induced by ZP, ACh, or PNU is almost completely prevented in α7nAChR-null sperm (Fig. 1*D*). These data clearly indicate that α7nAChR mediates the AR via enhancement of Ca^{2+} influx. Moreover, phorbol 12-myristate 13-acetate, which activates the downstream effector PKC, or 8-Br-cAMP, which activates PKA and Epac, also could not induce AR in α7nAChR-null sperm (Fig. 1*D*). These data indicate that sperm α7nAChR is crucial for the occurrence of AR, and the process cannot be bypassed by activating downstream effectors. The fact that the Ca^{2+}-ionophore can induce significant

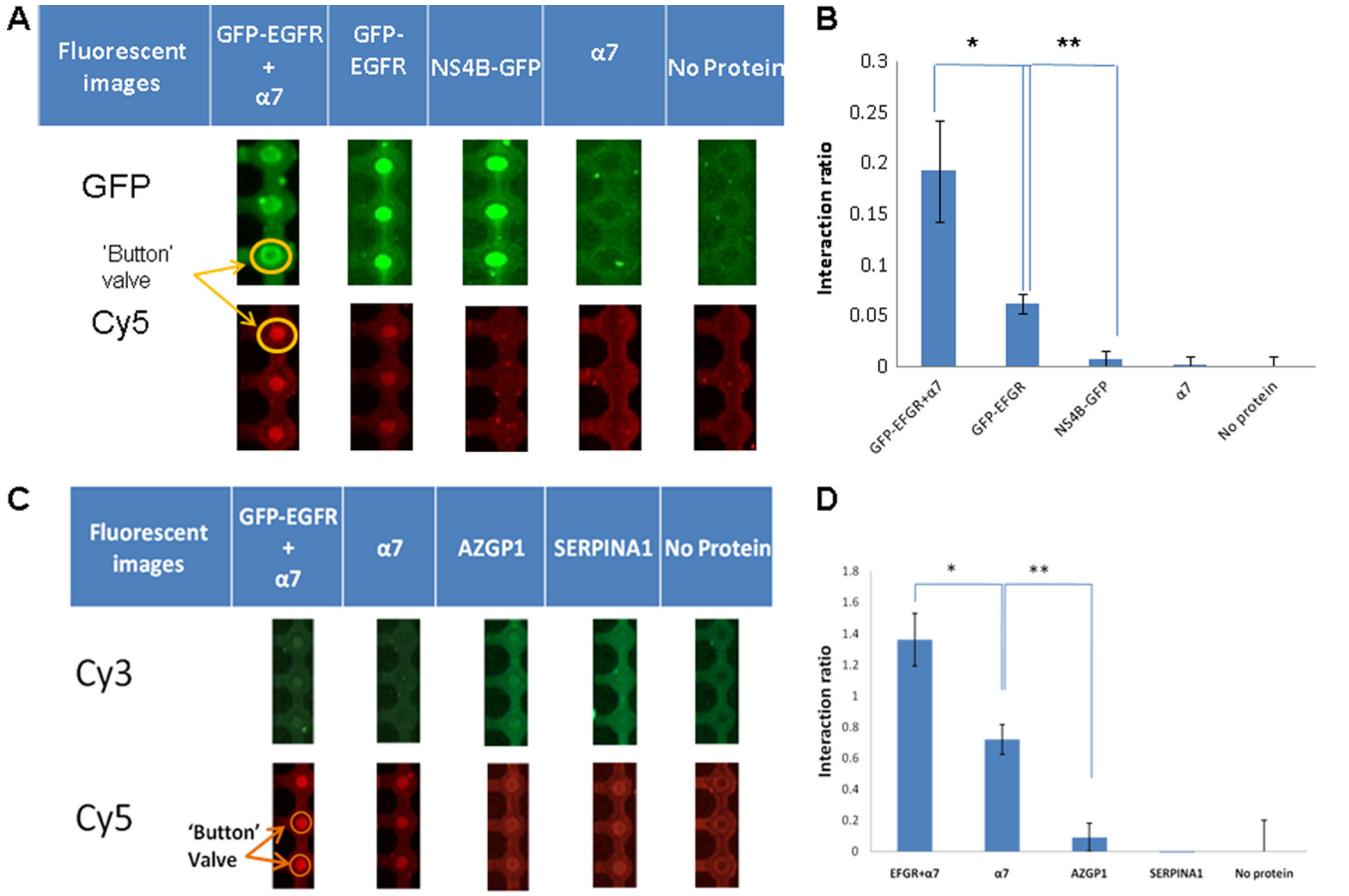

FIGURE 8. **Protein expression and protein-protein interactions.** *A*, fluorescent images from a microfluidic chip. EGFR and HCV-NS4B fused to GFP and α7 contain a C-Myc tag for measuring expression and a His tag for protein pulldown. The proteins were expressed in a tube, flowed inside the device, and anchored under the button valve using an α-GFP antibody. ZP3, which included a T7 tag for detecting interactions, was flowed over the pulled down proteins (EGFR and HCV-NS4B) and labeled with anti-T7-Cy5 antibody to detect protein interactions. *B*, the interactions are represented as the ratio between ZP3 intensity and the intensity of the surface-bound proteins (GFP-EGFR+α7, GFP-EGFR, α7, and NS4B). *, ZP3 interaction with the EGFR·α7 complex is significantly higher than with EGFR alone ($p < 0.0001$). **, ZP3 interaction with EGFR is much higher than with the control proteins ($p < 0.0001$) ($n = 40$). *C*, fluorescent images from a microfluidic chip. α7, AZGP1, and SERPINA1 contain a C-Myc tag for measuring expression and a His tag for protein pulldown. The proteins were expressed in a tube, flowed inside the device, anchored under the button valve using an α-His antibody, and labeled with α-C-Myc Cy3 antibody. ZP3, which includes a T7 tag for detecting interactions, was flowed over the pulled down proteins (α7, AZGP1, and SERPINA1) and labeled with anti-T7 Cy5 antibody to detect protein interactions. *D*, the interactions are represented as the ratio between ZP3 intensity and the intensity of the surface-bound proteins (EGFR+α7, AZGP1, and SERPINA1). *, ZP3 interaction with the EGFR·α7 complex is significantly higher than with α7 alone ($p = 3 \times 10^{-8}$); **, ZP3 interaction with α7 is much higher than with the control proteins ($p = 7 \times 10^{-15}$) ($n = 40$).

AR in α7nAChR-null sperm further supports α7nAChR mediation of Ca^{2+} influx and also proves that the Ca^{2+} influx mechanism in α7nAChR-null sperm is blocked but the AR mechanism works normally. And indeed, we have shown that PNU282987 or isolated ZP enhanced Ca^{2+} influx into WT sperm; however in α7nAChR-null sperm, Ca^{2+} influx induced by ZP or PNU were 40 or 90% inhibited, respectively (Fig. 3). The result, that Ca^{2+} influx induced by ZP is only 40% inhibited in α7nAChR-null sperm, suggests an alternative pathway for Ca^{2+} transport activated by ZP; however activating this mechanism is not enough to induce AR (Fig. 1, *A*, *B*, and *D*). The IVF rate was 45 or 30% inhibited in sperm originated from α7nAChR-null mice or treated with α-BgT, respectively, not corresponding with the ability to bind to the egg, which was almost completely blocked in α-BgT-treated sperm or in sperm originated in α7nAChR-null mice compared with the WT (Table 1). These data indicate the necessity for the sperm α7nAChR to recognize and fertilize the egg. The relatively low inhibition of the IVF rate can be explained by the fact that only one sperm cell is required for fertilization, and the one cell that bound to the egg is the most potent cell that could also fertilize.

It is known that in other cell types α7nAChR is capable of activating signal transduction pathways that do not involve the channel activity of the receptor (71, 72). Among the signal transducers, it can activate the PLCγ/PI3K and ERK1/2 two pathways known to be involved in sperm AR (57, 73, 74). Other work from this laboratory shows that PI3K is activated in sperm capacitation and can be activated by the EGFR (57). In the present study we show that EGFR also participates in AR induced by ZP or PNU. We found (Fig. 4*A*) that AG1478, a specific inhibitor of EGFR, inhibits the AR induced by ZP or PNU, indicating the involvement of EGFR in this process, activated by ZP or by α7nAChR. Furthermore, EGF could not induce the AR (Fig. 4*B*) or Ca^{2+} influx (Fig. 4*D*) in α7nAChR-null sperm compared with the WT. Moreover, we have shown here for the first time increased phosphorylation of EGFR (Tyr-845) in response to isolated ZP or PNU282987, an increase that was not observed in α7-null sperm (Fig. 5*A*). Moreover, this phosphorylation was

inhibited by α-BgT or by the SFK inhibitor PP1 (Fig. 5*B*). Taken together, these data indicate that activation of α7nAChR leads to the activation of EGFR, and in the absence of sperm α7nAChR the physiological process is damaged. To our surprise, however, AR induced by EGF was not affected by inhibition of α7nAChR using α-BgT or MLA (Fig. 4*C*); the EGF-induced AR was significantly reduced in α7nAChR-null sperm (Fig. 4*B*). Thus, we conclude that α7nAChR must be present in the sperm cell to achieve EGF-induced AR or to activate the EGFR. Indeed our data show very low EGF-induced EGFR phosphorylation/activation in α7-null sperm (Fig. 5*A*). Moreover, no staining of EGFR in the acrosome region of α7-null sperm could be detected (Fig. 7*A*), suggesting that α7nAChR is important for EGFR localization to the sperm head. The fact that the two receptors co-immunoprecipitated (Fig. 7*B*), along with the reduced effect of EGF on AR, Ca^{2+} influx and EGFR phosphorylation in α7nAChR-null sperm, suggests that a possible interaction between the two receptors is necessary for the activation of the EGFR to promote fertilization. Further support for the involvement of EGFR in the mechanism of ZP-induced Ca^{2+} influx is seen in Fig. 4*D*, where AG1478 inhibits the ZP effect.

In our recent study we showed that Src mediates EGFR activation induced by PKA activation (50). Here we show that PP1, a specific inhibitor of SFKs, blocked AR induced by PNU282987 or ZP by 80%, suggesting that SFKs mediates this reaction (Fig. 6*A*). It was not expected to find 40% inhibition by PP1 of EGF-induced AR, because theoretically there is no need for Src when EGFR is activated directly by EGF. Thus, we assume that Src also may be active downstream to EGFR in the AR mechanism. Evidence for this hypothesis is provided in Fig. 6*B*, which shows phosphorylation of Src in response to ZP, PNU, or EGF. The activation of Src by ZP, PNU, or EGF in the WT but not in α7nAChR-null sperm clearly indicates that the presence of α7nAChR in the sperm is obligatory for Src activation. Moreover, Src can be activated by activating α7nAChR or EGFR, and vice versa, the activation of Src leads to EGFR activation (Fig. 5*B*). Taken together, these data clearly indicate that activating α7nAChR leads to EGFR activation mediated by Src family kinase, which is also activated upon EGFR activation. Additionally, it has been shown elsewhere that α7nAChR and Src also form a complex in sperm cells (24, 37).

To support this mechanism, localization of these two receptors was conducted. Indeed Fig. 7*A* shows that α7nAChR and also the EGFR both localize to the acrosome region in WT sperm. Surprisingly, in α7nAChR-null sperm, the EGFR was not found in the acrosome but only in the mid-piece, which may indicate an anchoring role for α7nAChR in the sperm cells for signal transducers such as the EGFR and/or Src that are important for AR and the fertilization process. This could also explain the fact that in α7nAChR-null sperm AR was not induced by downstream effectors (Fig. 1*D*) or by EGFR activation, because of the lack of EGFR in the acrosome region where it can regulate the AR. The co-immunoprecipitation of α7nAChR and EGFR (Fig. 7*B*) further support a role for α7nAChR in regulating the EGFR.

To provide unequivocal evidence that α7nAChR and/or EGFR are the receptors recognized by the egg, a microfluidic affinity assay was conducted. Fig. 8 shows that α7nAChR and EGFR can bind separately to the egg ZP3; when they are expressed together the binding is twice as strong. This kind of evidence is provided here first regarding the fertility initiation process and sperm-egg recognition. Several sperm receptors have been characterized as the possible binding site for the egg ZP (55). The notion stands behind it is that several receptors that bind to the ZP enhance the efficiency of sperm-egg interaction and fertilization (67). We have suggested here that α7nAChR and the EGFR are sperm receptors that bind to the egg ZP3. The fact that α7nAChR-null sperm or α-BgT-treated sperm showed very low binding to the egg (Table 1), as well as the reduced IVF rate in α7nAChR-null sperm, strongly supports this notion.

In conclusion, in this study we have provided new information regarding the mechanism of the acrosome reaction and fertilization processes. In the suggested mechanism we show for the first time the requirement for α7nAChR in the AR, which activates the EGFR through Src activation, as well as a requirement for Ca^{2+} channel activity of α7nAChR. We found that in the absence of this receptor, intracellular calcium elevation and thus the acrosome reaction, as well as EGFR anchoring to the acrosome region and EGFR and Src activation, cannot occur. Furthermore, we found that Src and EGFR are activated by ZP, the physiological AR inducer, and that this activation depends on the presence of α7nAChR in the sperm. α7nAChR-null sperm can bind to the egg ZP in a very low rate, emphasizing the role of α7nAChR and its necessity for efficient sperm-egg interaction leading to normal fertilization. The data clearly indicate that α7nAChR and the EGFR are new suggested sperm receptors for ZP3.

REFERENCES

1. Jin, M., Fujiwara, E., Kakiuchi, Y., Okabe, M., Satouh, Y., Baba, S. A., Chiba, K., and Hirohashi, N. (2011) Most fertilizing mouse spermatozoa begin their acrosome reaction before contact with the zona pellucida during *in vitro* fertilization. *Proc. Natl. Acad. Sci. U.S.A.* **108,** 4892–4896
2. Florman, H. M., Tombes, R. M., First, N. L., and Babcock, D. F. (1989) An adhesion-associated agonist from the zona pellucida activates G protein-promoted elevations of internal $Ca2^{+}$ and pH that mediate mammalian sperm acrosomal exocytosis. *Dev. Biol.* **135,** 133–146
3. Arnoult, C., Zeng, Y., and Florman, H. (1996) ZP3-dependent activation of sperm cation channels regulates acrosomal secretion during mammalian fertilization. *J. Cell Biol.* **134,** 637–645
4. Fukami, K., Yoshida, M., Inoue, T., Kurokawa, M., Fissore, R. A., Yoshida, N., Mikoshiba, K., and Takenawa, T. (2003) Phospholipase Cδ4 is required for $Ca2^{+}$ mobilization essential for acrosome reaction in sperm. *J. Cell Biol.* **161,** 79–88
5. Shirakawa, H., and Miyazaki, S. (1999) Spatiotemporal characterization of intracellular $Ca2^{+}$ rise during the acrosome reaction of mammalian spermatozoa induced by zona pellucida. *Dev. Biol.* **208,** 70–78
6. Arnoult, C., Kazam, I. G., Visconti, P. E., Kopf, G. S., Villaz, M., and Florman, H. M. (1999) Control of the low voltage-activated calcium channel of mouse sperm by egg ZP3 and by membrane hyperpolarization during capacitation. *Proc. Natl. Acad. Sci. U.S.A.* **96,** 6757–6762
7. Treviño, C. L., Felix, R., Castellano, L. E., Gutiérrez, C., Rodríguez, D., Pacheco, J., López-González, I., Gomora, J. C., Tsutsumi, V., Hernández-Cruz, A., Fiordelisio, T., Scaling, A. L., and Darszon, A. (2004) Expression and differential cell distribution of low-threshold $Ca(2^{+})$ channels in mammalian male germ cells and sperm. *FEBS Lett.* **563,** 87–92
8. Jimenez-Gonzalez, C., Michelangeli, F., Harper, C. V., Barratt, C. L., and Publicover, S. J. (2006) Calcium signalling in human spermatozoa: a spe-

cialized "toolkit" of channels, transporters, and stores. *Hum. Reprod. Update* **12,** 253–267
9. Florman, H. M., and Ducibella, T. (2006) Fertilization in mammals, in *Physiology of Reproduction* (Neill, J. D., ed) pp. 55–112, Elsevier, San Diego
10. Publicover, S., Harper, C. V., and Barratt, C. (2007) $[Ca2^+]_i$ signalling in sperm: making the most of what you've got. *Nat. Cell Biol.* **9,** 235–242
11. Escoffier, J., Boisseau, S., Serres, C., Chen, C. C., Kim, D., Stamboulian, S., Shin, H. S., Campbell, K. P., De Waard, M., and Arnoult, C. (2007) Expression, localization, and functions in acrosome reaction and sperm motility of Ca(V)3.1 and Ca(V)3.2 channels in sperm cells: an evaluation from Ca(V)3.1 and Ca(V)3.2-deficient mice. *J. Cell Physiol.* **212,** 753–763
12. Chen, C. C., Lamping, K. G., Nuno, D. W., Barresi, R., Prouty, S. J., Lavoie, J. L., Cribbs, L. L., England, S. K., Sigmund, C. D., Weiss, R. M., Williamson, R. A., Hill, J. A., and Campbell, K. P. (2003) Abnormal coronary function in mice deficient in α1H T-type $Ca2^+$ channels. *Science* **302,** 1416–1418
13. Jungnickel, M. K., Marrero, H., Birnbaumer, L., Lémos, J. R., and Florman, H. M. (2001) Trp2 regulates entry of $Ca2^+$ into mouse sperm triggered by egg ZP3. *Nat. Cell Biol.* **3,** 499–502
14. O'Toole, C. M., Arnoult, C., Darszon, A., Steinhardt, R. A., and Florman, H. M. (2000) $Ca(2^+)$ entry through store-operated channels in mouse sperm is initiated by egg ZP3 and drives the acrosome reaction. *Mol. Biol. Cell* **11,** 1571–1584
15. Stowers, L., Holy, T. E., Meister, M., Dulac, C., and Koentges, G. (2002) Loss of sex discrimination and male-male aggression in mice deficient for TRP2. *Science* **295,** 1493–1500
16. Hogg, R. C., Raggenbass, M., and Bertrand, D. (2003) Nicotinic acetylcholine receptors: from structure to brain function. *Rev. Physiol. Biochem. Pharmacol.* **147,** 1–46
17. Millar, N. S. (2003) Assembly and subunit diversity of nicotinic acetylcholine receptors. *Biochem. Soc. Trans.* **31,** 869–874
18. Mitsui, T., Kawajiri, M., Kunishige, M., Endo, T., Akaike, M., Aki, K., and Matsumoto, T. (2000) Functional association between nicotinic acetylcholine receptor and sarcomeric proteins via actin and desmin filaments. *J. Cell. Biochem.* **77,** 584–595
19. Frail, D. E., McLaughlin, L. L., Mudd, J., and Merlie, J. P. (1988) Identification of the mouse muscle 43,000-dalton acetylcholine receptor-associated protein (RAPsyn) by cDNA cloning. *J. Biol. Chem.* **263,** 15602–15607
20. Kassner, P. D., Conroy, W. G., and Berg, D. K. (1998) Organizing effects of rapsyn on neuronal nicotinic acetylcholine receptors. *Mol. Cell. Neurosci.* **10,** 258–270
21. Ferns, M., Deiner, M., and Hall, Z. (1996) Agrin-induced acetylcholine receptor clustering in mammalian muscle requires tyrosine phosphorylation. *J. Cell Biol.* **132,** 937–944
22. Fuhrer, C., Sugiyama, J. E., Taylor, R. G., and Hall, Z. W. (1997) Association of muscle-specific kinase MuSK with the acetylcholine receptor in mammalian muscle. *EMBO J.* **16,** 4951–4960
23. Swope, S. L., Qu, Z., and Huganir, R. L. (1995) Phosphorylation of the nicotinic acetylcholine receptor by protein tyrosine kinases. *Ann. N.Y. Acad. Sci.* **757,** 197–214
24. Charpantier, E., Wiesner, A., Huh, K. H., Ogier, R., Hoda, J. C., Allaman, G., Raggenbass, M., Feuerbach, D., Bertrand, D., and Fuhrer, C. (2005) α7 neuronal nicotinic acetylcholine receptors are negatively regulated by tyrosine phosphorylation and Src-family kinases. *J. Neurosci.* **25,** 9836–9849
25. Berg, D. K., and Conroy, W. G. (2002) Nicotinic α7 receptors: synaptic options and downstream signaling in neurons. *J. Neurobiol.* **53,** 512–523
26. Suzuki, T., Hide, I., Matsubara, A., Hama, C., Harada, K., Miyano, K., Andrä, M., Matsubayashi, H., Sakai, N., Kohsaka, S., Inoue, K., and Nakata, Y. (2006) Microglial α7 nicotinic acetylcholine receptors drive a phospholipase C/IP3 pathway and modulate the cell activation toward a neuroprotective role. *J. Neurosci. Res.* **83,** 1461–1470
27. Placzek, R., Krassnigg, F., and Schill, W. B. (1988) Effect of ace-inhibitors, calmodulin antagonists, acetylcholine receptor blocking, and α receptor blocking agents on motility of human sperm. *Arch. Androl.* **21,** 1–10
28. Nelson, L. (1976) α-Bungarotoxin binding by cell membranes. Blockage of sperm cell motility. *Exp. Cell Res.* **101,** 221–224
29. Young, R. J., and Laing, J. C. (1991) The binding characteristics of cholinergic sites in rabbit spermatozoa. *Mol. Reprod. Dev.* **28,** 55–61
30. Stewart, T. A., and Forrester, I. T. (1978) Acetylcholinesterase and choline acetyltransferase in ram spermatozoa. *Biol. Reprod.* **19,** 271–279
31. Ibáñez, C. F., Pelto-Huikko, M., Söder, O., Ritzèn, E. M., Hersh, L. B., Hökfelt, T., and Persson, H. (1991) Expression of choline acetyltransferase mRNA in spermatogenic cells results in an accumulation of the enzyme in the postacrosomal region of mature spermatozoa. *Proc. Natl. Acad. Sci. U.S.A.* **88,** 3676–3680
32. Stewart, T. A., and Forrester, I. T. (1978) Identification of a cholinergic receptor in ram spermatozoa. *Biol. Reprod.* **19,** 965–970
33. Bray, C., Son, J. H., and Meizel, S. (2002) A nicotinic acetylcholine receptor is involved in the arosome reaction of human sperm initiated by recombinant human ZP3. *Biol. Reprod.* **67,** 782–788
34. Son, J. H., and Meizel, S. (2003) Evidence suggesting that the mouse sperm acrosome reaction initiated by the zona pellucida involves an α7 nicotinic acetylcholine receptor. *Biol. Reprod.* **68,** 1348–1353
35. Bray, C., Son, J. H., Kumar, P., and Meizel, S. (2005) Mice deficient in CHRNA7, a subunit of the nicotinic acetylcholine receptor, produce sperm with impaired motility. *Biol. Reprod.* **73,** 807–814
36. Bray, C., Son, J. H., and Meizel, S. (2005) Acetylcholine causes an increase of intracellular calcium in human sperm. *Mol. Hum. Reprod.* **11,** 881–889
37. Kumar, P., and Meizel, S. (2005) Nicotinic acetylcholine receptor subunits and associated proteins in human sperm. *J. Biol. Chem.* **280,** 25928–25935
38. Shoop, R. D., Yamada, N., and Berg, D. K. (2000) Cytoskeletal links of neuronal acetylcholine receptors containing α7 subunits. *J. Neurosci.* **20,** 4021–4029
39. Brener, E., Rubinstein, S., Cohen, G., Shternall, K., Rivlin, J., and Breitbart, H. (2003) Remodeling of the actin cytoskeleton during mammalian sperm capacitation and acrosome reaction. *Biol. Reprod.* **68,** 837–845
40. Cohen, G., Rubinstein, S., Gur, Y., and Breitbart, H. (2004) Crosstalk between protein kinase A and C regulates phospholipase D and F-actin formation during sperm capacitation. *Dev. Biol.* **267,** 230–241
41. Citri, A., and Yarden, Y. (2006) EGF-ERBB signalling: towards the systems level. *Nat. Rev. Mol. Cell Biol.* **7,** 505–516
42. Sibilia, M., Kroismayr, R., Lichtenberger, B. M., Natarajan, A., Hecking, M., and Holcmann, M. (2007) The epidermal growth factor receptor: from development to tumorigenesis. *Differentiation* **75,** 770–787
43. Wieduwilt, M. J., and Moasser, M. M. (2008) The epidermal growth factor receptor family: biology driving targeted therapeutics. *Cell. Mol. Life Sci.* **65,** 1566–1584
44. Ferguson, K. M. (2008) Structure-based view of epidermal growth factor receptor regulation. *Annu. Rev. Biophys.* **37,** 353–373
45. Schneider, M. R., and Wolf, E. (2009) The epidermal growth factor receptor ligands at a glance. *J. Cell. Physiol.* **218,** 460–466
46. Jorissen, R. N., Walker, F., Pouliot, N., Garrett, T. P., Ward, C. W., and Burgess, A. W. (2003) Epidermal growth factor receptor: mechanisms of activation and signalling. *Exp. Cell Res.* **284,** 31–53
47. Prenzel, N., Zwick, E., Daub, H., Leserer, M., Abraham, R., Wallasch, C., and Ullrich, A. (1999) EGF receptor transactivation by G-protein-coupled receptors requires metalloproteinase cleavage of proHB-EGF. *Nature* **402,** 884–888
48. Shah, B. H., and Catt, K. J. (2003) A central role of EGF receptor transactivation in angiotensin II-induced cardiac hypertrophy. *Trends Pharmacol. Sci.* **24,** 239–244
49. Wetzker, R., and Böhmer, F. D. (2003) Transactivation joins multiple tracks to the ERK/MAPK cascade. *Nat. Rev. Mol. Cell Biol.* **4,** 651–657
50. Etkovitz, N., Tirosh, Y., Chazan, R., Jaldety, Y., Daniel, L., Rubinstein, S., and Breitbart, H. (2009) Bovine sperm acrosome reaction induced by G-protein-coupled receptor agonists is mediated by epidermal growth factor receptor transactivation. *Dev. Biol.* **334,** 447–457
51. Sánchez-González, P., Jellali, K., and Villalobo, A. (2010) Calmodulin-mediated regulation of the epidermal growth factor receptor. *FEBS J.* **277,** 327–342
52. Lax, Y., Rubinstein, S., and Breitbart, H. (1994) Epidermal growth factor induces acrosomal exocytosis in bovine sperm. *FEBS Lett.* **339,** 234–238
53. Nair, V. D., and Sealfon, S. C. (2003) Agonist-specific transactivation of phosphoinositide 3-kinase signaling pathway mediated by the dopamine D2 receptor. *J. Biol. Chem.* **278,** 47053–47061
54. Visconti, P. E., Bailey, J. L., Moore, G. D., Pan, D., Olds-Clarke, P., and Kopf, G. S. (1995) Capacitation of mouse spermatozoa. I. Correlation be-

tween the capacitation state and protein tyrosine phosphorylation. *Development* **121,** 1129–1137
55. Ward, C. R., and Kopf, G. S. (1993) Molecular events mediating sperm activation. *Dev. Biol.* **158,** 9–34
56. Bleil, J. D., and Wassarman, P. M. (1986) Autoradiographic visualization of the mouse egg's sperm receptor bound to sperm. *J. Cell Biol.* **102,** 1363–1371
57. Etkovitz, N., Rubinstein, S., Daniel, L., and Breitbart, H. (2007) Role of PI3-kinase and PI4-kinase in actin polymerization during bovine sperm capacitation. *Biol. Reprod.* **77,** 263–273
58. Fordyce, P. M., Gerber, D., Tran, D., Zheng, J., Li, H., DeRisi, J. L., and Quake, S. R. (2010) *De novo* identification and biophysical characterization of transcription factor-binding sites with microfluidic affinity analysis. *Nat. Biotechnol.* **28,** 970–975
59. Einav, S., Gerber, D., Bryson, P. D., Sklan, E. H., Elazar, M., Maerkl, S. J., Glenn, J. S., and Quake, S. R. (2008) Discovery of a hepatitis C target and its pharmacological inhibitors by microfluidic affinity analysis. *Nat. Biotechnol.* **26,** 1019–1027
60. Gerber, D., Maerkl, S. J., and Quake, S. R. (2009) An *in vitro* microfluidic approach to generating protein-interaction networks. *Nat. Methods* **6,** 71–74
61. Bódis, J., Koppán, M., Kornya, L., Tinneberg, H. R., and Török, A. (2002) The effect of catecholamines, acetylcholine, and histamine on progesterone release by human granulosa cells in a granulosa cell superfusion system. *Gynecol. Endocrinol.* **16,** 259–264
62. Kornya, L., Bódis, J., Koppán, M., Tinneberg, H. R., and Török, A. (2001) Modulatory effect of acetylcholine on gonadotropin-stimulated human granulosa cell steroid secretion. *Gynecol. Obstet. Invest.* **52,** 104–107
63. Mayerhofer, A., Frungieri, M. B., Bulling, A., and Fritz, S. (1999) *Medicina (B Aires)* **59,** 542–545
64. Meizel, S., and Son, J. H. (2005) Studies of sperm from mutant mice suggesting that two neurotransmitter receptors are important to the zona pellucida-initiated acrosome reaction. *Mol. Reprod. Dev.* **72,** 250–258
65. Hajós, M., Hurst, R. S., Hoffmann, W. E., Krause, M., Wall, T. M., Higdon, N. R., and Groppi, V. E. (2005) The selective α7 nicotinic acetylcholine receptor agonist PNU-282987 [*N*-[(3*R*)-1-azabicyclo[2.2.2]oct-3-yl]-4-chlorobenzamide hydrochloride] enhances GABAergic synaptic activity in brain slices and restores auditory gating deficits in anesthetized rats. *J. Pharmacol. Exp. Ther.* **312,** 1213–1222
66. Yoshimatsu, N., Yanagimachi, R., and Lopata, A. (1988) Zonae pellucidae of salt-stored hamster and human eggs: their penetrability by homologous and heterologous spermatozoa. *Gamete Res.* **21,** 115–126
67. Lyng, R., and Shur, B. D. (2007) Sperm-egg binding requires a multiplicity of receptor-ligand interactions: new insights into the nature of gamete receptors derived from reproductive tract secretions. *Soc. Reprod. Fertil. Suppl.* **65,** 335–351
68. Daniel, L., Etkovitz, N., Weiss, S. R., Rubinstein, S., Ickowicz, D., and Breitbart, H. (2010) Regulation of the sperm EGF receptor by ouabain leads to initiation of the acrosome reaction. *Dev. Biol.* **344,** 650–657
69. Mitchell, L. A., Nixon, B., Baker, M. A., and Aitken, R. J. (2008) Investigation of the role of SRC in capacitation-associated tyrosine phosphorylation of human spermatozoa. *Mol. Hum. Reprod.* **14,** 235–243
70. Florman, H. M., Jungnickel, M. K., and Sutton, K. A. (2008) Regulating the acrosome reaction. *Int. J. Dev. Biol.* **52,** 503–510
71. Blanchet, M. R., Israël-Assayag, E., Daleau, P., Beaulieu, M. J., and Cormier, Y. (2006) Dimethyphenylpiperazinium, a nicotinic receptor agonist, down-regulates inflammation in monocytes/macrophages through PI3K and PLC chronic activation. *Am. J. Physiol. Lung Cell. Mol. Physiol.* **291,** L757–L763
72. de Jonge, W. J., and Ulloa, L. (2007) The α7 nicotinic acetylcholine receptor as a pharmacological target for inflammation. *Br. J. Pharmacol.* **151,** 915–929
73. Breitbart, H., Rotman, T., Rubinstein, S., and Etkovitz, N. (2010) Role and regulation of PI3K in sperm capacitation and the acrosome reaction. *Mol. Cell. Endocrinol.* **314,** 234–238
74. Almog, T., Lazar, S., Reiss, N., Etkovitz, N., Milch, E., Rahamim, N., Dobkin-Bekman, M., Rotem, R., Kalina, M., Ramon, J., Raziel, A., Breitbart, H., Seger, R., and Naor, Z. (2008) Identification of extracellular signal-regulated kinase 1/2 and p38 MAPK as regulators of human sperm motility and acrosome reaction and as predictors of poor spermatozoan quality. *J. Biol. Chem.* **283,** 14479–14489